

1 **COVID-19 ARDS is characterized by a dysregulated host response that differs from**  
2 **cytokine storm and is modified by dexamethasone**

3

4 **Authors:**

5 Aartik Sarma<sup>1</sup>, Stephanie A. Christenson<sup>1</sup>, Eran Mick<sup>1,2,3</sup>, Catherine DeVoe<sup>2</sup>, Thomas Deiss<sup>2</sup>,  
6 Angela Oliveira Pisco<sup>3</sup>, Rajani Ghale<sup>1,2</sup>, Alejandra Jauregui<sup>2</sup>, Ashley Byrne<sup>3</sup>, Farzad Moazed<sup>1</sup>,  
7 Natasha Spottiswoode<sup>4</sup>, Pratik Sinha<sup>5</sup>, Beth Shoshana Zha<sup>1</sup>, Norma Neff<sup>3</sup>, Michelle Tan<sup>3</sup>, Paula  
8 Hayakawa Serpa<sup>2,3</sup>, K. Mark Ansel<sup>7,8</sup>, Jennifer G. Wilson<sup>9</sup>, Aleksandra Leligdowicz<sup>2</sup>, Emily R.  
9 Siegel<sup>10</sup>, Marina Sirota<sup>11</sup>, Joseph L. DeRisi<sup>3,6</sup>, Michael A. Matthay<sup>1</sup>, COMET Consortium<sup>†</sup>,  
10 Carolyn M. Hendrickson<sup>1</sup>, Kirsten N. Kangelaris<sup>4</sup>, Matthew F. Krummel<sup>12</sup>, Prescott G.  
11 Woodruff<sup>1,8</sup>, David J. Erle<sup>4,13,14</sup>, \*Carolyn S. Calfee<sup>1</sup>, \*\*Charles R. Langelier<sup>2,3</sup>

12 \* These authors contributed equally

13

14 **Affiliations**

15 <sup>1</sup> Division of Pulmonary, Critical Care, Allergy, and Sleep Medicine, University of California, San  
16 Francisco, CA, USA

17 <sup>2</sup> Division of Infectious Diseases, University of California, San Francisco, CA, USA

18 <sup>3</sup> Chan Zuckerberg Biohub, San Francisco, CA, USA

19 <sup>4</sup> Department of Medicine, University of California, San Francisco, CA, USA

20 <sup>5</sup> Department of Anesthesia, Washington University, Saint Louis, Missouri, MO, USA

21 <sup>6</sup> Department of Biochemistry and Biophysics, University of California, San Francisco, CA, USA

22 <sup>7</sup> Department of Microbiology and Immunology, University of California, San Francisco, CA, USA

23 <sup>8</sup> Sandler Asthma Basic Research Center, University of California, San Francisco, CA, USA

24 <sup>9</sup> Department of Emergency Medicine, Stanford University, Palo Alto, CA, USA

25 <sup>10</sup> School of Medicine, University of California, San Francisco, CA, USA

26 <sup>11</sup> Division of Rheumatology, University of California, San Francisco, CA, USA

27 <sup>12</sup> Department of Pathology, University of California, San Francisco, CA, USA

28 <sup>13</sup> Lung Biology Center, University of California, San Francisco, CA, USA

29 <sup>14</sup> UCSF CoLabs, University of California, San Francisco, CA, USA

30 <sup>†</sup>COMET (COVID-19 Multiphenotyping for Effective Therapies) Consortium members are listed  
31 in the Supplementary Appendix.

32

33 <sup>‡</sup> Correspondence: [chaz.langelier@ucsf.edu](mailto:chaz.langelier@ucsf.edu)

34

35

36 **Keywords:** COVID-19, RNA-seq, transcriptomics, ARDS, cytokine storm, SARS-CoV-2,  
37 coronavirus, metagenomics

38

39 **Word Count:** 2665

40

41 **Funding**

42 NIH R35 HL140026 (CSC), NIH/NIAID U19 AI1077439 (DE), NHLBI K23HL138461-01A1 (CL),

43 K24HL137013 (PGW), F32 HL151117 (AS), Chan Zuckerberg Biohub (AOP, AB, JLD).

44 **Abstract**

45 We performed comparative lower respiratory tract transcriptional profiling of 52 critically ill  
46 patients with the acute respiratory distress syndrome (ARDS) from COVID-19 or from other  
47 etiologies, as well as controls without ARDS. In contrast to a cytokine storm, we observed  
48 reduced proinflammatory gene expression in COVID-19 ARDS when compared to ARDS due to  
49 other causes. COVID-19 ARDS was characterized by a dysregulated host response with  
50 increased PTEN signaling and elevated expression of genes with non-canonical roles in  
51 inflammation and immunity that were predicted to be modulated by dexamethasone and  
52 granulocyte colony stimulating factor. Compared to ARDS due to other types of viral pneumonia,  
53 COVID-19 was characterized by impaired interferon-stimulated gene expression (ISG). We found  
54 that the relationship between SARS-CoV-2 viral load and expression of ISGs was decoupled in  
55 patients with COVID-19 ARDS when compared to patients with mild COVID-19. In summary,  
56 assessment of host gene expression in the lower airways of patients with COVID-19 ARDS did  
57 not demonstrate cytokine storm but instead revealed a unique and dysregulated host response  
58 predicted to be modified by dexamethasone.

## 60 **Introduction**

61 In its most severe form, coronavirus disease 2019 (COVID-19) can precipitate the acute  
62 respiratory distress syndrome (ARDS), which is characterized by low arterial oxygen  
63 concentrations, alveolar injury and a dysregulated inflammatory response in the lungs<sup>1</sup>. Early  
64 reports hypothesized that COVID-19 ARDS was driven by a “cytokine storm” based on the  
65 detection of higher circulating inflammatory cytokine levels in critically ill COVID-19 patients  
66 compared to those with mild disease or healthy controls<sup>2-4</sup>. Recent studies, however, have found  
67 that patients with COVID-19 ARDS in fact have lower plasma cytokine levels compared to those  
68 with ARDS due to other causes<sup>5</sup>, highlighting a need to understand the underlying mechanisms  
69 of COVID-19 ARDS.

70 Clinical trials have demonstrated a significant mortality benefit for dexamethasone in  
71 COVID-19 patients with ARDS<sup>6</sup>, implicating a role for dysregulated inflammation in COVID-19  
72 pathophysiology given the immunomodulatory effects of corticosteroids. In contrast, clinical trials  
73 of corticosteroids for ARDS prior to the SARS-CoV-2 pandemic have had mixed results, ranging  
74 from benefit to possible harm<sup>1</sup>. These differences suggest distinct biology in COVID-19 ARDS,  
75 with important implications for pathogenesis and treatment.

76 While several studies have assessed host airway transcriptional responses to SARS-  
77 CoV-2<sup>7,8</sup>, none have compared COVID-19 ARDS to other causes of ARDS. We hypothesized  
78 that this comparison would identify distinct biological features of SARS-CoV-2 related lung injury  
79 and tested this by evaluating lower respiratory tract gene expression in critically ill adults.

80

## 81 **Results**

82 We conducted a prospective case-control study of 52 adults requiring mechanical  
83 ventilation (**Table 1**) for ARDS from COVID-19 (COVID-ARDS, n= 15), ARDS from other  
84 etiologies (Other-ARDS, n= 32), or for airway protection in the absence of pulmonary disease  
85 (No-ARDS, n = 5). Other ARDS etiologies included pneumonia, aspiration, sepsis, and  
86 transfusion reaction. Patients were enrolled at two tertiary care hospitals in San Francisco,

87 California under research protocols approved by the University of California San Francisco  
88 Institutional Review Board (**Methods**). We excluded immunosuppressed patients to avoid  
89 confounding the measurement of host inflammatory responses (**Methods**). Tracheal aspirate  
90 (TA) was collected within five days of intubation and underwent RNA sequencing (**Methods**).

91 We compared TA gene expression between COVID-ARDS and Other-ARDS patients  
92 (**Methods, Fig. 1a, Supplementary Data 2**) and identified 696 differentially expressed genes at  
93 an adjusted P-value < 0.1, as well as differentially activated pathways using Ingenuity Pathway  
94 Analysis (IPA)<sup>9</sup>. Notably, we did not observe elevated expression of genes encoding canonical  
95 proinflammatory cytokines, such as IL-1 or IL-6, in COVID-ARDS compared to Other-ARDS. In  
96 fact, IL-1, IL-6 and several other cytokine signaling pathways were more highly activated in  
97 Other-ARDS, whereas COVID-ARDS patients had comparable inflammatory pathway activation  
98 to No-ARDS controls (**Fig. 1b, Supplementary Data 3**). We also found attenuation of the  
99 proinflammatory HIF-1a and nitric oxide signaling pathways in COVID-ARDS compared to Other-  
100 ARDS patients. To relate these lower respiratory tract findings to systemic inflammatory  
101 responses, we also assessed circulating plasma cytokines. We found no difference in IL-6 or IL-  
102 8 levels, and lower concentrations of sTNFR1, in COVID-ARDS versus Other-ARDS patients  
103 (**Fig. 1c, Supplementary Data 4**).

104 Evaluation of genes with the most significant expression differences in COVID-ARDS  
105 compared to Other-ARDS did, however, reveal several differences in genes regulating immunity  
106 and inflammation (**Supplementary Data 2**). For instance, among genes upregulated in COVID-  
107 ARDS, *P2RY14* functions in purinergic receptor signaling to mediate inflammatory responses  
108 and its ligand UDP-glucose promotes neutrophil recruitment in the lung<sup>10</sup>. Conversely, *ARG1*,  
109 which promotes macrophage efferocytosis and inflammation resolution<sup>11</sup>, was downregulated in  
110 COVID-ARDS versus Other-ARDS patients.

111 At the pathway level, we observed activation of PTEN signaling in COVID-ARDS  
112 compared to both Other-ARDS and No-ARDS patients (**Fig. 1b, Supplementary Data 3**). PTEN  
113 modulates both innate and adaptive immune responses by opposing the activity of PI3K<sup>12</sup>.

114 Consistent with our observations, PTEN attenuates expression of certain cytokines while  
115 amplifying other innate immune responses in a manner that may promote injurious inflammation  
116 during respiratory infections<sup>13</sup>, suggesting a potentially pathologic role in COVID-ARDS. *In silico*  
117 prediction of cell type composition (**Methods, Supplementary Fig. 1, Supplementary Data 5**)  
118 did not identify differences in lymphocyte, macrophage or neutrophil populations but did identify  
119 markedly decreased proportions of type-2 alveolar epithelial cells and increased proportions of  
120 goblet and ciliated cells in COVID-ARDS compared to Other-ARDS. This may reflect alveolar  
121 epithelial injury, airway remodeling, and/or preferential SARS-CoV-2 infection of cells with the  
122 highest expression of *ACE2* and *TMPRSS2*<sup>14</sup>.

123 To test the hypothesis that existing pharmaceuticals might counter the dysregulated  
124 transcriptional signature of COVID-19 related ARDS, we compared differentially expressed  
125 genes against the IPA database of 12,981 drug treatment-induced transcriptional signatures  
126 derived from human studies and cell culture experiments<sup>9</sup> (**Methods, Fig. 1c, Supplementary**  
127 **Data 6**). Dexamethasone was the compound predicted to most significantly counter-regulate the  
128 genes expressed in COVID-ARDS patients compared to No-ARDS patients, and was also  
129 significant with respect to the Other-ARDS group. This finding was striking given that  
130 dexamethasone is the only drug thus far proven to confer a mortality benefit in patients with  
131 severe COVID-19<sup>6</sup>. Granulocyte colony stimulating factor (G-CSF) was also significant, which is  
132 intriguing given that a recent clinical trial found a mortality benefit in COVID-19 patients treated  
133 with this agent<sup>15</sup>. Other corticosteroids (fluticasone, prednisolone) as well as omega-3 fatty acids  
134 (eicosapentenoic and docosahexaenoic acids) were also predicted to counteract the  
135 transcriptional profile of COVID-ARDS with respect to comparator groups and thus may  
136 represent possible therapeutic agents (**Fig. 1c, Supplementary Data 6**).

137 As our analysis did not reveal evidence of a cytokine storm in COVID-19 ARDS, we  
138 hypothesized that other steroid-responsive pathways may be responsible for the therapeutic  
139 benefit of dexamethasone. Although commonly thought of as indiscriminate immunosuppressive  
140 medications, glucocorticoids affect diverse biological processes. We therefore proceeded to

141 examine the genes comprising the transcriptional signature of COVID-ARDS that were also  
142 predicted to be regulated by dexamethasone (**Supplementary Data 7**). Interestingly, both  
143 dexamethasone and G-CSF were predicted to attenuate the expression of several genes highly  
144 upregulated in COVID-ARDS versus controls (e.g., *P2YR14*) as well as other genes with well-  
145 established roles in immunity, inflammation, and interferon responses. For instance, we found  
146 that COVID-ARDS patients had increased expression of the interferon-inducible and  
147 dexamethasone-regulated gene *EPSTI1*, which promotes M1 macrophage polarization<sup>16</sup>, and  
148 *STAT1*, which induces chemokine expression, regulates differentiation of hematopoietic cells,  
149 and promotes reactive oxygen species production<sup>17</sup>.

150 ARDS is a heterogeneous syndrome caused by diverse infectious and non-infectious  
151 insults<sup>1</sup>. To more precisely understand host response relationships between subtypes of ARDS,  
152 we performed secondary analyses comparing the transcriptional signature of COVID-ARDS  
153 without co-infections (n = 8) to that of ARDS caused exclusively by other viral (n = 4, **Fig. 2a**,  
154 **Supplementary Data 1**) or bacterial (n = 9, **Fig. 2b**) lower respiratory tract infections (LRTI)  
155 (**Supplementary Data 8**). COVID-ARDS was characterized by lower expression of  
156 proinflammatory signaling pathways compared to bacterial LRTI-associated ARDS (**Fig. 2c**,  
157 **Supplementary Data 9**), but higher levels of the same pathways compared to viral LRTI-  
158 associated ARDS.

159 Although interferon-related gene expression was higher in COVID-ARDS compared to  
160 bacterial LRTIs and no-ARDS controls, it was markedly attenuated in ARDS patients with  
161 COVID-19 versus those with other viral LRTI (**Fig. 2d**, **Supplementary Data 10**, **Methods**). Prior  
162 studies found strong correlation between SARS-CoV-2 viral load and expression of interferon-  
163 stimulated genes (ISGs) in the upper respiratory tract of patients with mild disease, early during  
164 infection<sup>18</sup>. In contrast, in the lower respiratory tract of patients with severe disease, we  
165 observed decoupling of this relationship for several ISGs (**Figs. 2e-f**, **Supplementary Data 11**),  
166 suggesting that a dysregulated interferon response in the lower respiratory tract may  
167 characterize severe COVID-19. This hypothesis is supported by recent findings of impaired

168 interferon signaling in peripheral blood immune cells of patients with severe versus mild COVID-  
169 19<sup>19</sup>, and a recent report suggesting that a dysregulated interferon response may be a universal  
170 characteristic of severe viral infections<sup>20</sup>.

171

## 172 **Discussion**

173 Our results challenge the cytokine storm model of COVID-19 ARDS. Instead, we observe  
174 a complex picture of host immune dysregulation that includes upregulation of genes with non-  
175 canonical roles in inflammation, immunity and interferon signaling that are predicted to be  
176 attenuated by dexamethasone, G-CSF and other potential therapeutics. Our work emphasizes  
177 the value of including clinically relevant control patients in COVID-19 immunophenotyping studies  
178 and underscores that detection of elevated cytokine levels in the blood does not necessarily  
179 equate to causality in pathogenesis. Single cytokine blockade was attempted unsuccessfully in  
180 the past for treatment of sepsis<sup>21</sup>, which like COVID-19, is characterized by dysregulated host  
181 response to infection as well as significant biologically meaningful heterogeneity<sup>22</sup>.

182 This work also builds on recent reports of dysregulated interferon responses in patients  
183 with severe COVID-19 pneumonia and suggests that decoupling of viral load from interferon  
184 signaling may be a relevant pathologic feature of severe disease. Further work in a larger cohort  
185 that also includes direct measurement of cytokine levels in the lower airway will be needed to  
186 validate these results. In conclusion, comparative lower respiratory transcriptional profiling of  
187 patients with ARDS did not find evidence of a COVID-19 related cytokine storm but did reveal a  
188 unique dysregulated host response predicted to be moderated by dexamethasone and other  
189 potential therapeutics.



190 **Materials and Methods**

191

192 Study design, clinical cohort and ethics statement

193 We conducted a case-control study of patients with ARDS due to COVID-19 (n = 15)  
194 versus two control groups of either patients with ARDS due to other causes (n = 32) or patients  
195 intubated for airway protection without evidence of pulmonary pathology on imaging (n = 5). We  
196 studied patients who were enrolled in either of two prospective cohort studies of critically ill  
197 patients at the University of California, San Francisco (UCSF) and Zuckerberg San Francisco  
198 General Hospital. Both studies were approved by the UCSF Institutional Review Board  
199 according under protocols 17-24056 and 20-30497, respectively, which granted a waiver of  
200 initial consent for tracheal aspirate and blood sampling. Informed consent was subsequently  
201 obtained from patients or their surrogates for continued study participation, as previously  
202 described<sup>23</sup>.

203 For this analysis, inclusion criteria were: 1) admission to the intensive care unit for  
204 mechanical ventilation for ARDS or airway protection, 2) age  $\geq$  18 years, 3) availability of TA  
205 with  $10^6$  protein-coding reads collected within five days of intubation. Exclusion criteria were: 1)  
206 receipt of immunosuppressive medication or underlying immunocompromising condition prior to  
207 tracheal aspirate collection. Subject charts and chest x-rays were reviewed by at least two study  
208 authors (AS, PS, ES, FM, CD, MM, CL, CC) to confirm a diagnosis of ARDS using the Berlin  
209 Definition<sup>24</sup>. Lower respiratory tract infections were adjudicated by two study physicians using  
210 the United States Centers for Disease Control surveillance definition of pneumonia<sup>25</sup>. Of 72  
211 patients initially screened, nine with ARDS due to COVID-19 and 10 with ARDS due to other  
212 causes were excluded because of treatment with immunosuppressant medications or because  
213 of an underlying immunocompromising condition (e.g., solid organ transplantation, bone marrow  
214 transplantation, human immunodeficiency virus infection).

215

216 Metagenomic sequencing

217           Following enrollment, TA was collected and mixed 1:1 with DNA/RNA shield (Zymo  
218 Research) to preserve nucleic acid. To evaluate host gene expression and detect the presence  
219 of SARS-CoV-2 and other viruses, metagenomic next generation sequencing (mNGS) of RNA  
220 was performed on TA specimens. Following RNA extraction (Zymo Pathogen Magbead Kit) and  
221 DNase treatment, human cytosolic and mitochondrial ribosomal RNA was depleted using  
222 FastSelect (Qiagen). To control for background contamination, we included negative controls  
223 (water and HeLa cell RNA) as well as positive controls (spike-in RNA standards from the  
224 External RNA Controls Consortium (ERCC))<sup>26</sup>. RNA was then fragmented and underwent library  
225 preparation using the NEBNext Ultra II RNAseq Kit (New England Biolabs). Libraries underwent  
226 146 nucleotide paired-end Illumina sequencing on an Illumina Novaseq 6000 instrument.

227

228 Host differential expression and pathway analysis

229           Following demultiplexing, sequencing reads were pseudo-aligned with kallisto<sup>27</sup> (v.  
230 0.46.1; including bias correction) to an index consisting of all transcripts associated with human  
231 protein coding genes (ENSEMBL v. 99), cytosolic and mitochondrial ribosomal RNA sequences,  
232 and the sequences of ERCC RNA standards. Samples retained in the dataset had a total of at  
233 least 1,000,000 estimated counts associated with transcripts of protein coding genes, and the  
234 median across all samples was 7.3 million. Gene-level counts were generated from the  
235 transcript-level abundance estimates using the R package tximport<sup>28</sup>, with the scaledTPM  
236 method.

237           Differential expression analysis was performed using DESeq2<sup>29</sup>. We modeled the  
238 expression of individual genes using the design formula ~ARDSEtiology. In our primary  
239 analysis, the ARDS etiology was categorized as COVID-ARDS, Other-ARDS, or No-ARDS. In  
240 our secondary analysis, the ARDS etiology was categorized as COVID-ARDS, Viral-ARDS,  
241 Bacterial-ARDS, or No-ARDS. COVID-ARDS patients with viral or bacterial co-infections were

242 excluded from this secondary analysis. Significant genes were identified using an independent-  
243 hypothesis-weighted, Benjamini-Hochberg false discovery rate (FDR) less than 0.1<sup>30,31</sup>.  
244 Empirical Bayesian adaptive shrinkage estimators for log<sub>2</sub>-fold change were fit using *ashr*<sup>32</sup>. We  
245 generated heatmaps of the top 50 differentially expressed genes by absolute log<sub>2</sub>-fold change.  
246 For visualization, gene expression was normalized using the variance stabilizing transformation,  
247 centered, and z-scaled. Heatmaps were generated using the *pheatmap* package. Patients were  
248 clustered using Euclidean distance and genes were clustered using Manhattan distance.  
249 Differentially expressed genes (FDR < 0.1) were analyzed using Ingenuity Pathway Analysis  
250 (IPA, Qiagen)<sup>9,33</sup>.

251

#### 252 Canonical pathway analysis and drug/cytokine upstream regulator analysis

253 To evaluate signaling pathways and upstream transcriptional regulators from gene  
254 expression data, we employed IPA. Specifically, genes were analyzed using Core, Canonical  
255 Pathway and Upstream Regulator Analysis on shrunken log<sub>2</sub>-fold change. IPA Upstream  
256 Regulator Analysis was employed to identify potential drug and cytokine regulators and predict  
257 their activation states based on expected effects between regulators and their known target  
258 genes or proteins annotated in the Ingenuity Knowledge Base (IKB)<sup>33</sup>. IPA calculates a Fisher's  
259 exact p-value for overlap of differentially expressed genes with curated gene sets representing  
260 canonical biological pathways, or upstream regulators of gene expression, including cytokines  
261 and 12,981 drugs. In addition, IPA calculates a Z-score for the direction of gene expression for a  
262 pathway or regulator based on the observed gene expression in the dataset. The Z-score  
263 signifies whether expression changes for genes within pathways, or for known target genes of  
264 upstream regulators, are consistent with what is expected based on previously published  
265 analyses annotated in the IKB. Significant pathways and upstream regulators were defined as  
266 those with a Z-score absolute value greater than 2 and an overlap P value < 0.05.

267

268 In silico analysis of cell type proportions

269 Cell-type proportions were estimated from bulk host transcriptome data using the  
270 CIBERSORT X algorithm<sup>34</sup>. We used the Human Lung Cell Atlas dataset<sup>35</sup> to derive the single  
271 cell signatures. The cell types estimated with this reference cover all expected cell types in the  
272 airway. The estimated proportions were compared between the three patient groups using a  
273 Mann-Whitney-Wilcoxon test (two-sided) with Bonferroni correction.

274

275 Quantification of SARS-CoV-2 viral load by mNGS

276 All samples were processed through a SARS-CoV-2 reference-based assembly pipeline  
277 that involved removing reads likely originating from the human genome or from other viral  
278 genomes annotated in RefSeq with Kraken2 (v. 2.0.8\_beta), and then aligning the remaining  
279 reads to the SARS-CoV-2 reference genome MN908947.3 using minimap2 (v. 2.17). We  
280 calculated SARS-CoV-2 reads-per-million (rpM) by dividing the number of reads that aligned to  
281 the virus with mapq  $\geq 20$  by the total number of reads in the sample (excluding reads mapping to  
282 ERCC RNA standards).

283

284 Regression of ISG counts against viral load in TA and NP samples

285 We assembled a set of 100 interferon-stimulated genes based on the “Hallmark  
286 interferon alpha response” gene set in MSigDB<sup>36</sup>. We then performed robust regression of the  
287 quantile normalized gene counts ( $\log_2$  scale), generated using the R package *limma*, against  
288  $\log_{10}(\text{rpM})$  of SARS-CoV-2. This was done in two separate datasets of COVID-19 patients: i) the  
289 tracheal aspirate (TA) samples from patients with COVID-19 ARDS reported in this study  
290 (n=15); and ii) the nasopharyngeal swab (NP) samples from patients with mostly early and mild  
291 disease that we previously reported (n=93)<sup>18</sup>. The analysis was performed using the R package  
292 robustbase (v. 0.93.6), which implements MM-type estimators for linear regression. Model  
293 predictions were generated using the R package ggeffects (v. 0.14.3) and used for display in the

294 individual gene plots. Error bands represent normal distribution 95% confidence intervals  
295 around each prediction. Reported P-values for significance of the difference of the regression  
296 coefficient from 0 are based on a t-statistic and Benjamini-Hochberg adjusted. Reported R<sup>2</sup>  
297 values represent the adjusted robust coefficient of determination.

298

### 299 **Data and Code Availability**

300 Human gene counts for the samples generated in this study can be obtained under  
301 NCBI GEO accession GSE163426. The published human lung single-cell datasets<sup>37</sup> used for  
302 cell type proportions analysis can be obtained through Synapse under accessions syn21560510  
303 and syn21560511. Code for the differential expression and cell type proportions analysis is  
304 available at: <https://github.com/AartikSarma/COVIDARDS>.

305

### 306 **Acknowledgements**

307 This study was performed with support from the National Institute of Allergy and  
308 Infectious Diseases-sponsored Immunophenotyping Assessment in a COVID-19 Cohort  
309 (IMPACC) Network. We gratefully appreciate support from Amy Kistler, PhD, Jack Kamm, PhD,  
310 Angela Deitweiller, PhD, Saharai Caldera, BS and Maira Phelps BS. We thank Mark and Carrie  
311 Casey, Julia and Kevin Hartz, Carl Kawaja and Wendy Holcombe, Eric Keisman and Linda  
312 Nevin, Martin and Leesa Romo, Three Sisters Foundation, Diana Wagner and Jerry Yang and  
313 Akiko Yamazaki for their support.

314

### 315 **Author Contributions**

316 CRL, CSC, AS and SC conceived and designed the study. TD, RG, PHS, NN, MT and KMA  
317 oversaw or performed sample processing, library preparation and sequencing. CSC, CMH, KNK  
318 RG, AJ, JGW and ERS coordinated or contributed to clinical operations including patient  
319 enrollment. CD, AS, CRL, FM, TD and NS performed metadata collation or clinical chart review.

320 AS, EM, AOP, CRL and SAC performed data analysis and interpretation. CSC, SAC, EM, DJE,  
321 JLD, KMA, MFK, PFW, MAM, BSZ, JGW, AL, AB, FM, PS and MS provided guidance, advice  
322 and comments on the study design and manuscript. CRL, AS and CSC wrote the manuscript  
323 with input from all authors.

325 **Table 1.** Clinical and demographic characteristics of patients with ARDS due to COVID-19  
 326 (COVID-ARDS), control patients with ARDS due to other etiologies (Other-ARDS), and intubated  
 327 control patients without ARDS (No-ARDS).

	<b>COVID-ARDS</b>	<b>Other-ARDS</b>	<b>P</b>	<b>No-ARDS</b>	<b>P</b>
<b>N</b>	15	32		5	
<b>Age (median [IQR])</b>	54.8 [42.5, 67.5]	61.4 [47.3, 71.5]	0.205	66.2 [62.0, 82.0]	0.190
<b>Male</b>	9 (60.0)	20 (62.5)	1.000	2 (40.0)	0.795
<b>30-day mortality</b>	3 (20.0)	11 (34.4)	0.508	2 (40.0)	0.546
<b>Race (%)</b>			<0.001		0.029
African American	0 (0.0)	2 (6.2)		0 (0.0)	
Asian	3 (20.0)	4 (12.5)		1 (20.0)	
Caucasian	1 (6.7)	23 (71.9)		3 (60.0)	
Other	11 (73.3)	3 (9.4)		1 (20.0)	
<b>Hispanic ethnicity</b>	8 (53.3)	3 (9.4)	0.003	0 (0.0)	0.114
<b>PaO<sub>2</sub>/FiO<sub>2</sub> (median [IQR])*</b>	74.0 [60.5, 115.0]	96.0 [67.0, 148.0]	0.114	296.0 [216.0, 366.5]	0.003
<b>ARDS etiology (%)</b>			0.109		<0.001
Aspiration	0 (0.0)	5 (15.6)		0 (0.0)	
LRTI	15 (100.0)	20 (62.5)		0 (0.0)	
Sepsis	0 (0.0)	4 (12.5)		0 (0.0)	
Transfusion	0 (0.0)	2 (6.2)		0 (0.0)	
Unknown	0 (0.0)	1 (3.1)		0 (0.0)	
None	0 (0.0)	0 (0.0)		5 (100.0)	
<b>LRTI type (%)</b>			<0.001		<0.001
Bacterial	0 (0.0)	9 (28.1)		0 (0.0)	
Viral	8 (60.0)	4 (12.5)		0 (0.0)	
Viral + Bacterial	4 (20.0)	3 (9.4)		0 (0.0)	
Viral + Viral	3 (20.0)	0 (0.0)		0 (0.0)	
Unknown	0 (0.0)	4 (12.5)		0 (0.0)	
None	0 (0.0)	12 (37.5)		5 (100.0)	

P-values represent comparisons versus COVID-ARDS. Reasons for intubation of No-ARDS patients included: hemorrhagic stroke, subdural hematoma, retroperitoneal hemorrhage or other neurosurgical procedure. Statistical significance was determined using Fisher's exact test (discrete variables) or by Wilcoxon test (continuous variables). \*Lowest PaO<sub>2</sub>/FiO<sub>2</sub> recorded in first five days of mechanical ventilation. PF ratios were not available for two Other-ARDS subjects, who were diagnosed with ARDS based on an SaO<sub>2</sub>/FiO<sub>2</sub> < 315. IQR = Interquartile Range.

328

329

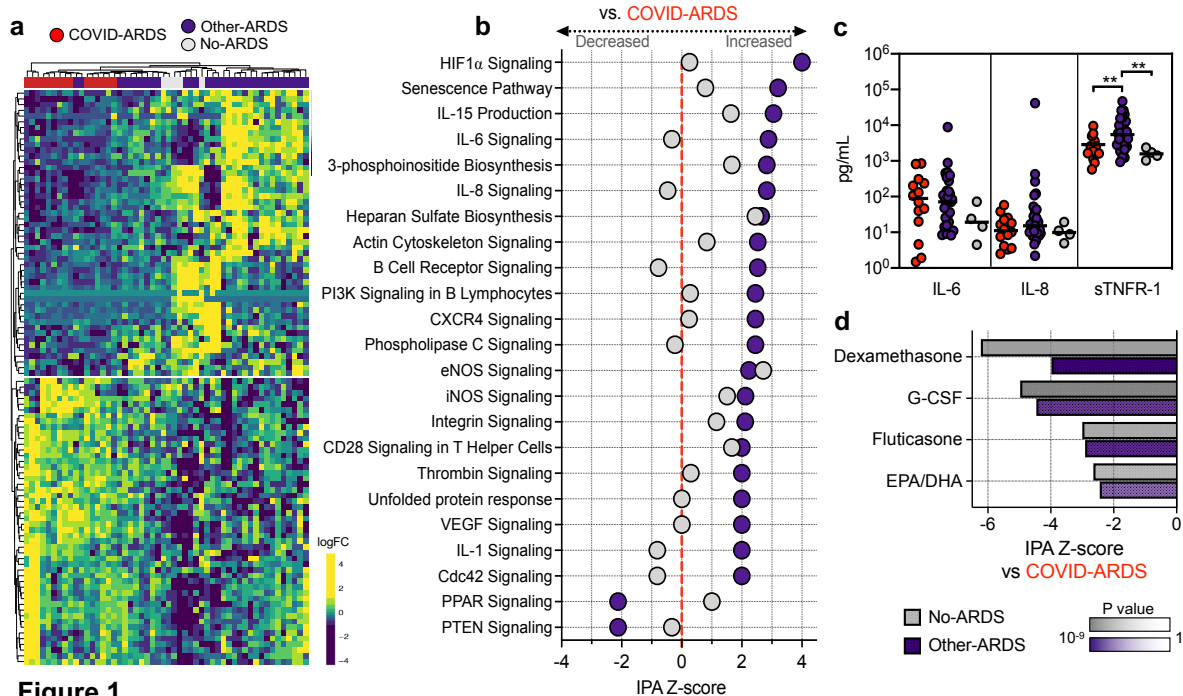


**Figure 1**

330  
331

332 **Figure 1.** Lower respiratory tract transcriptional signature of COVID-19 ARDS. **a)** Heatmap of the  
333 top 50 differentially expressed genes by adjusted p value between patients with COVID-19  
334 related ARDS (COVID-ARDS, red) versus controls with ARDS due to other etiologies (Other-  
335 ARDS, violet). Intubated controls with no ARDS were also included in the unsupervised  
336 clustering (No-ARDS, grey). **b)** Ingenuity Pathway Analysis (IPA) based on differential gene  
337 expression analyses demonstrating expression of signaling pathways by IPA activation Z-score  
338 with respect to a baseline of COVID-ARDS. Values are tabulated in (Supplementary Data 3). **c)**  
339 Differences in plasma inflammatory cytokine concentrations between patients with ARDS due to  
340 COVID-19 (COVID-ARDS, red) or other etiologies (Other-ARDS, violet). Lines indicate medians.  
341 P values calculated based on Mann-Whitney test. Values tabulated in (Supplementary Data 4).  
342 **d)** Pharmacologic agents predicted to mitigate the dysregulated host response of COVID-19  
343 ARDS with respect to Other-ARDS (violet) or No-ARDS patients (grey) identified by  
344 computational matching against the IPA database of drug transcriptional signatures. Values  
345 tabulated in (Supplementary Data 5). Pathways with a Z-score absolute value > 2 and overlap P  
346 value < 0.05 are significant.



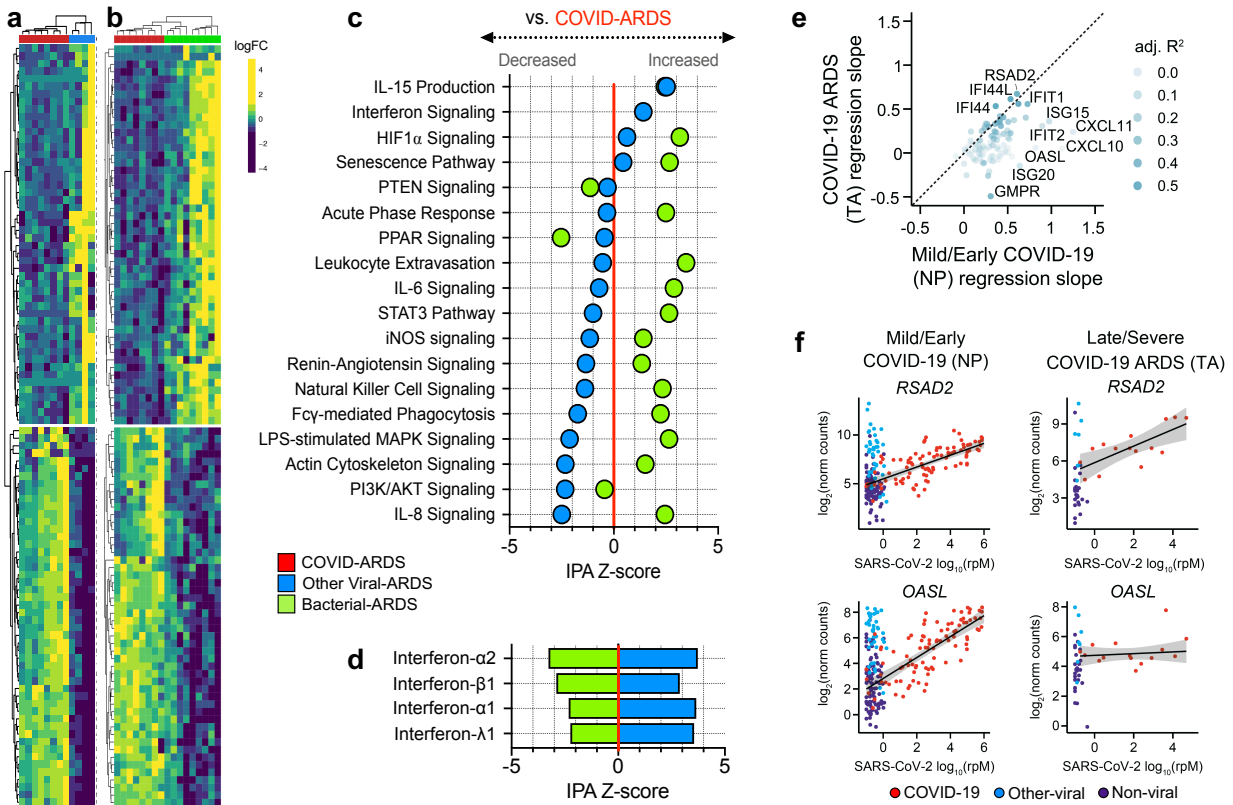


**Figure 2**

347  
348  
349  
350  
351  
352  
353  
354  
355  
356  
357  
358  
359  
360  
361  
362  
363  
364  
365  
366  
367  
368  
369

**Figure 2.** Lower respiratory tract transcriptional signature of ARDS due to COVID-19 versus other viral or bacterial lower respiratory tract infections. **a)** Heatmap depicting expression and unsupervised clustering of top differentially expressed genes by adjusted P value between patients with COVID-19 related ARDS (COVID-ARDS, red) versus ARDS due to viral LRTI (Viral-ARDS, blue). **b)** Heatmap depicting expression and unsupervised clustering of the top 50 differentially expressed genes between patients with COVID-19 related ARDS (COVID-ARDS, red) versus ARDS due to bacterial LRTI (Bacterial-ARDS, green). **c)** Pathway analysis based on differentially expressed genes depicting relative expression of signaling pathways by IPA Z-score with respect to a baseline of gene expression in COVID-ARDS. Values are tabulated in (Supplementary Data 8). **d)** Predicted activation of upstream interferons in patients with ARDS due to viral or bacterial LRTI compared to those with COVID-ARDS revealed downregulation of type-I/III interferons in COVID-ARDS versus other viral LRTI-related ARDS. Values tabulated in (Supplementary Data 9). **e)** Scatterplot of the relationship between interferon-stimulated gene (ISG) counts and SARS-CoV-2 viral load (reads per million, rpM), quantified by the regression slope, in nasopharyngeal (NP) samples from patients with mostly mild/early COVID-19 (x-axis) and in tracheal aspirate (TA) samples from patients with severe COVID-19 and ARDS (y-axis). **f)** *RSAD2* is an ISG whose expression (y-axis) is correlated with SARS-CoV-2 viral load (x-axis) in both early/mild (NP) and severe (TA) disease, while *OASL* is an ISG for which the correlation observed in early/mild COVID-19 is absent in severe COVID-19 patients with ARDS. Values are tabulated in (Supplementary Data 10).

370 **References**

- 371 1. Matthay, M. A. *et al.* Acute respiratory distress syndrome. *Nature Reviews Disease Primers*  
372 **5**, (2019).
- 373 2. Mehta, P. *et al.* COVID-19: consider cytokine storm syndromes and immunosuppression.  
374 *The Lancet* **395**, 1033–1034 (2020).
- 375 3. Blanco-Melo, Daniel. Imbalanced host response to SARS-CoV-2 drives development of  
376 COVID-19. *Cell*. doi:10.1016/j.cell.2020.04.026.
- 377 4. Giamarellos-Bourboulis, E. J. *et al.* Complex Immune Dysregulation in COVID-19 Patients  
378 with Severe Respiratory Failure. *Cell Host Microbe* **27**, 992-1000.e3 (2020).
- 379 5. Wilson, J. G. *et al.* Cytokine profile in plasma of severe COVID-19 does not differ from  
380 ARDS and sepsis. *JCI Insight* **5**, (2020).
- 381 6. The RECOVERY Collaborative Group. Dexamethasone in Hospitalized Patients with Covid-  
382 19 — Preliminary Report. *New England Journal of Medicine* (2020)  
383 doi:10.1056/NEJMoa2021436.
- 384 7. Bost, P. *et al.* Host-Viral Infection Maps Reveal Signatures of Severe COVID-19 Patients.  
385 *Cell* **181**, 1475-1488.e12 (2020).
- 386 8. Chua, R. L. *et al.* COVID-19 severity correlates with airway epithelium–immune cell  
387 interactions identified by single-cell analysis. *Nature Biotechnology* **38**, 970–979 (2020).
- 388 9. Krämer, A., Green, J., Pollard, J. & Tugendreich, S. Causal analysis approaches in  
389 Ingenuity Pathway Analysis. *Bioinformatics* **30**, 523–530 (2014).
- 390 10. Sesma, J. I. *et al.* UDP-glucose promotes neutrophil recruitment in the lung. *Purinergic*  
391 *Signalling* **12**, 627–635 (2016).
- 392 11. Cai, W. *et al.* STAT6/Arg1 promotes microglia/macrophage efferocytosis and inflammation  
393 resolution in stroke mice. *JCI Insight* **4**, (2019).
- 394 12. Chen, L. & Guo, D. The functions of tumor suppressor PTEN in innate and adaptive  
395 immunity. *Cellular & Molecular Immunology* **14**, 581–589 (2017).

- 396 13. Schabbauer, G. *et al.* Myeloid PTEN Promotes Inflammation but Impairs Bactericidal  
397 Activities during Murine Pneumococcal Pneumonia. *The Journal of Immunology* **185**, 468–  
398 476 (2010).
- 399 14. HCA Lung Biological Network *et al.* SARS-CoV-2 entry factors are highly expressed in  
400 nasal epithelial cells together with innate immune genes. *Nature Medicine* **26**, 681–687  
401 (2020).
- 402 15. Cheng, L. *et al.* Effect of Recombinant Human Granulocyte Colony–Stimulating Factor for  
403 Patients With Coronavirus Disease 2019 (COVID-19) and Lymphopenia: A Randomized  
404 Clinical Trial. *JAMA Internal Medicine* (2020) doi:10.1001/jamainternmed.2020.5503.
- 405 16. Kim, Y.-H., Lee, J.-R. & Hahn, M.-J. Regulation of inflammatory gene expression in  
406 macrophages by epithelial-stromal interaction 1 (Epsti1). *Biochem Biophys Res Commun*  
407 **496**, 778–783 (2018).
- 408 17. Kaplan, M. H. STAT signaling in inflammation. *JAK-STAT* **2**, e24198 (2013).
- 409 18. Mick, E. *et al.* Upper airway gene expression reveals suppressed immune responses to  
410 SARS-CoV-2 compared with other respiratory viruses. *Nature Communications* **11**, (2020).
- 411 19. Hadjadj, J. *et al.* Impaired type I interferon activity and inflammatory responses in severe  
412 COVID-19 patients. *Science* **369**, 718–724 (2020).
- 413 20. Zheng, H. *et al.* Multi-cohort analysis of host immune response identifies conserved  
414 protective and detrimental modules associated with severity irrespective of virus.  
415 <http://medrxiv.org/lookup/doi/10.1101/2020.10.02.20205880> (2020)  
416 doi:10.1101/2020.10.02.20205880.
- 417 21. Cavillon, J., Singer, M. & Skirecki, T. Sepsis therapies: learning from 30 years of failure of  
418 translational research to propose new leads. *EMBO Molecular Medicine* **12**, (2020).
- 419 22. Seymour, C. W. *et al.* Assessment of Clinical Criteria for Sepsis: For the Third International  
420 Consensus Definitions for Sepsis and Septic Shock (Sepsis-3). *JAMA* **315**, 762 (2016).

- 421 23. Langelier, C. *et al.* Integrating host response and unbiased microbe detection for lower  
422 respiratory tract infection diagnosis in critically ill adults. *Proc Natl Acad Sci USA* 201809700  
423 (2018) doi:10.1073/pnas.1809700115.
- 424 24. ARDS Definition Task Force. Acute respiratory distress syndrome: the Berlin definition.  
425 *JAMA* **307**, 2526–2533 (2012).
- 426 25. United States Centers for Disease Control and Prevention. CDC/NHSN Surveillance  
427 Definitions for Specific Types of Infections. (2017).
- 428 26. Pine, P. S. *et al.* Evaluation of the External RNA Controls Consortium (ERCC) reference  
429 material using a modified Latin square design. *BMC Biotechnology* **16**, 54 (2016).
- 430 27. Bray, N. L., Pimentel, H., Melsted, P. & Pachter, L. Near-optimal probabilistic RNA-seq  
431 quantification. *Nature Biotechnology* **34**, 525 (2016).
- 432 28. Sonesson, C., Love, M. I. & Robinson, M. D. Differential analyses for RNA-seq: transcript-  
433 level estimates improve gene-level inferences. *F1000Research* **4**, 1521 (2015).
- 434 29. Love, M. I., Huber, W. & Anders, S. Moderated estimation of fold change and dispersion for  
435 RNA-seq data with DESeq2. *Genome Biology* **15**, 550 (2014).
- 436 30. Ignatiadis, N., Klaus, B., Zaugg, J. B. & Huber, W. Data-driven hypothesis weighting  
437 increases detection power in genome-scale multiple testing. *Nature Methods* **13**, 577–580  
438 (2016).
- 439 31. Benjamini, Y. & Hochberg, Y. Controlling the False Discovery Rate: A Practical and  
440 Powerful Approach to Multiple Testing. *Journal of the Royal Statistical Society: Series B*  
441 (*Methodological*) **57**, 289–300 (1995).
- 442 32. Stephens, M. False discovery rates: a new deal. *Biostatistics* **18**, 275–294 (2017).
- 443 33. Ingenuity Systems. *Ingenuity Upstream Regulator Analysis in IPA*.  
444 [http://pages.ingenuity.com/rs/ingenuity/images/0812%20upstream\\_regulator\\_analysis\\_whit](http://pages.ingenuity.com/rs/ingenuity/images/0812%20upstream_regulator_analysis_whit)  
445 [epaper.pdf](http://pages.ingenuity.com/rs/ingenuity/images/0812%20upstream_regulator_analysis_whit).

- 446 34. Newman, A. M. *et al.* Robust enumeration of cell subsets from tissue expression profiles.  
447 *Nature methods* **12**, 453–457 (2015).
- 448 35. Travaglini, K. J. *et al.* A molecular cell atlas of the human lung from single-cell RNA  
449 sequencing. *Nature* **587**, 619–625 (2020).
- 450 36. Subramanian, A. *et al.* Gene set enrichment analysis: A knowledge-based approach for  
451 interpreting genome-wide expression profiles. *Proceedings of the National Academy of*  
452 *Sciences* **102**, 15545–15550 (2005).
- 453 37. Travaglini, K. J. *et al.* A molecular cell atlas of the human lung from single cell RNA  
454 sequencing. *bioRxiv* 742320 (2020) doi:10.1101/742320.

457 **Supplementary Materials**

458

459 **Supplementary Data 1.** Detailed clinical, microbiological and demographic features of the  
460 cohort. Legend: \*SaO<sub>2</sub>/FiO<sub>2</sub> Ratio (SF Ratio) < 315 was used to verify ARDS diagnosis in these  
461 subjects.

462

463 **Supplementary Data 2.** Differentially expressed genes (adjusted P value (padj) < 0.1) between  
464 patients with ARDS due to COVID-19 (COVID-ARDS) versus **a)** controls with ARDS due to  
465 other etiologies (Other-ARDS) or **b)** intubated controls without ARDS (No-ARDS). Positive fold  
466 change indicates gene is upregulated in COVID-ARDS.

467

468 **Supplementary Data 3.** Ingenuity Pathway Analysis (IPA) of differentially expressed genes  
469 (padj < 0.1) between patients with ARDS due to COVID-19 (COVID-ARDS) versus **a)** controls  
470 with ARDS due to other etiologies (Other-ARDS) or **b)** intubated controls without ARDS (No-  
471 ARDS). Positive Z-score indicates pathway is upregulated in COVID-ARDS. Pathways with a Z-  
472 score absolute value ≥ 1 are included in table.

473

474 **Supplementary Data 4.** Plasma concentrations of inflammatory cytokines in patients with  
475 ARDS due to COVID-19 (COVID-ARDS) versus controls with ARDS due to other etiologies  
476 (Other-ARDS).

477

478 **Supplementary Data 5.** *In silico* deconvolution of cell type proportions from tracheal aspirate  
479 bulk RNA-sequencing data using lung single cell signatures. Data are plotted in (Supplementary  
480 Figure 1).

481

482 **Supplementary Data 6.** Chemical and biological drugs computationally predicted by IPA to  
483 attenuate the transcriptional response of ARDS due to COVID-19 (COVID-ARDS) against a  
484 comparator group of **a)** ARDS due to other causes (Other-ARDS) or **b)** intubated controls  
485 without ARDS (No-ARDS). Drugs with a Z-score > 2 are included in table.

486

487 **Supplementary Data 7.** Genes affected by drugs computationally predicted by IPA to modulate  
488 the transcriptional response of ARDS due to COVID-19 (COVID-ARDS) against a comparator  
489 group of **a)** ARDS due to other causes (Other-ARDS) or **b)** intubated controls without ARDS  
490 (No-ARDS). Predicted transcriptional effect of each drug on each gene is indicated with respect  
491 to comparator group 1 in the table.

492

493 **Supplementary Data 8.** Differentially expressed genes ( $p_{adj} < 0.1$ ) between patients with  
494 ARDS due to COVID-19 (COVID-ARDS) versus controls with ARDS due to **a)** other viral lower  
495 respiratory tract infections (Other Viral-ARDS) or **b)** bacterial lower respiratory tract infections  
496 (Bacterial-ARDS). Positive  $\log_2$  fold change indicates gene is upregulated in COVID-ARDS.

497

498 **Supplementary Data 9.** Pathway analysis (IPA) of differentially expressed genes ( $p_{adj} < 0.1$ )  
499 between patients with ARDS due to COVID-19 (COVID-ARDS) versus controls with ARDS due  
500 to other viral or bacterial lower respiratory tract infections. Z-scores are with respect to COVID-  
501 ARDS. Pathways with a Z-score absolute value  $\geq 1$  are included in table.

502

503 **Supplementary Data 10.** Computationally predicted (IPA) upstream cytokines based on the  
504 transcriptional signature of COVID-19 ARDS (COVID-ARDS) compared to ARDS from other  
505 viral LRTI. Pathways with a Z-score absolute value  $\geq 1$  are included in table.

506

507 **Supplementary Data 11.** Relationship between interferon-stimulated gene (ISG) expression  
508 and SARS-CoV-2 viral load measured in RNA-seq reads per million (rpM) for COVID-19  
509 patients with late, severe disease and ARDS (COVID-ARDS) from lower respiratory tract  
510 samples (this study), and COVID-19 patients with early, mostly mild disease measured from  
511 upper respiratory tract samples<sup>18</sup>. Legend: reg\_intercept = intercept in the robust regression of  
512 gene expression on SARS-CoV-2 viral load; reg\_slope = slope in the robust regression of gene  
513 expression on SARS-CoV-2 viral load; reg\_adj\_R2 = adjusted robust coefficient of  
514 determination; reg\_p\_adj = Benjamini-Hochberg adjusted p-value for difference of the  
515 regression slope from 0.

516

517 **Supplementary Appendix.** COMET Consortium member list.

518

519 **Supplementary Figure 1.** *In silico* deconvolution of cell types from tracheal aspirate bulk RNA-  
520 sequencing data using lung single cell signatures. The horizontal line inside the box denotes the  
521 median and the lower and upper hinges correspond to the first and third quartiles, respectively.  
522 Whiskers extend from the hinge to the largest (smallest, respectively) value no more than  
523  $1.5 \times \text{IQR}$  away from the hinge, where IQR is the interquartile range. The y-axis in each panel  
524 was trimmed at the maximum value among the three patient groups of  $1.5 \times \text{IQR}$  above the third  
525 quartile. Pairwise comparisons between patient groups were performed with a two-sided Mann-  
526 Whitney-Wilcoxon test followed by Bonferroni's correction (n=15 COVID-ARDS, n=32 Other  
527 ARDS, n=5 No-ARDS). Data are tabulated in (Supplementary Data 5).



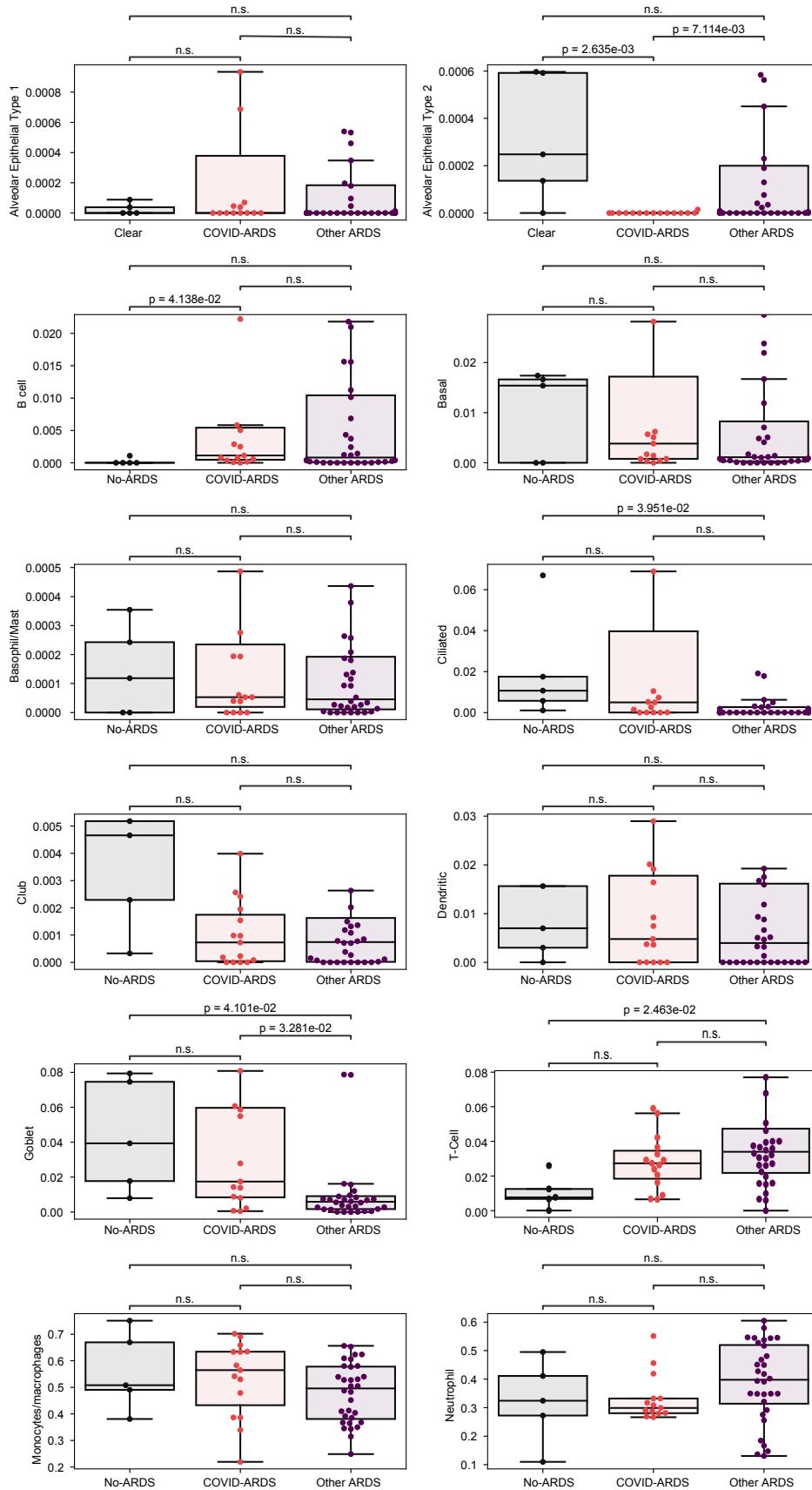


Figure S1